This article has been accepted for publication in a future issue of this journal, but has not been fully edited. Content may change prior to final publication. Citation information: DOI 10.1109/JSEN.2014.2331271, IEEE Sensors Journal

Optimum Power Allocation with Sensitivity Analysis for Passive Radar Applications

Gholamreza Alirezaei, *Student Member, IEEE,* Omid Taghizadeh, *Student Member, IEEE,* and Rudolf Mathar, *Member, IEEE*

***Abstract*—In the present paper, we investigate the power allocation problem in distributed sensor networks and give a sensitivity analysis for perfect and imperfect knowledge of system parameters. As it is common for sensors with weak power-supplies, constraints by sum and individual power-range limitations are imposed. The power allocation problem leads to a signomial program, and is analytically solved by a Lagrangian setup. Typical examples of such networks are passive radar systems with multiple nodes, whose aim is to detect and classify target signals. For each sensor node, an amplify-and-forward strategy for the received target signal is proposed. This per-node information is transmitted over a communication channel and combined at a fusion center. The fusion center carries out the final decision about the type of the target signal by a best linear unbiased estimator and a subsequent classification. In contrast to approaches in the literature, which combine discrete local decisions into a single global one, the approach in the current paper offers many advantages, ranging from the simplicity of its implementation to the achievement of an optimal solution in closed-form. Moreover, it allows for a sensitivity analysis of the whole sensor network under variations of different system parameters.**

***Index Terms*—Closed-form optimization, energy-efficient system-design, distributed radar, network resource management, information fusion.**

I. Introduction

DISTRIBUTED passive multiple-radar systems (DPMRS) are used for a variety of modern applications. Physicists use this type of radar to detect or to determine specific characteristics of particles, for example, in the neutrino telescope '*IceCube Neutrino Observatory*' at the Amundsen-Scott South Pole Station [2] in Antarctica, where a network with over 5000 nodes is implemented. They also use such radars for radio astronomy to study celestial objects, for instance in the '*Karl G. Jansky Very Large Array*' of the National Radio Astronomy Observatory [3] in Socorro County, New Mexico. Many other applications of DPMRSs are military [4] and some are also for civil usage [5]. Because of the importance of DPMRSs on the one hand, and power-sensitive nature of sensor nodes (SNs) on the other hand, an energy-aware design of the entire network is of high interest. The significance of this approach becomes more clear if considering individual powering mechanisms for sensor nodes constituted by weak batteries, intermittent power-supplies, or by inefficient energy conversion techniques. Especially, large sensor networks for space and extreme environment applications, where power consumption is a crucial element, require an energy-efficient operation. Thus, the task is to allocate power within the sensor network such that the radar accuracy is improved at a constant overall energy consumption [6]. The problem of finding an optimum power allocation for a distributed radar system in closed-form under certain constraints is extremely hard. The main difficulty lies in finding an explicit representation of the objective function, as mentioned in [7]. Recently, some novel methods have been proposed to solve the power allocation problem. In particular, the authors in [8] have investigated game-theoretic approaches to solve the power allocation problem not focussing on DPMRSs. The power allocation for localization purposes is investigated in [9], [10] and [11]. The capacity bound and the corresponding power allocation in a single relay system is considered in [12] and [13]. The optimal power allocation for an active radar instead of a passive radar system is given in [14]. Moreover, an optimum power allocation scheme for decode-and-forward parallel relay networks, instead of amplify-and-forward sensor networks, is investigated in [15].

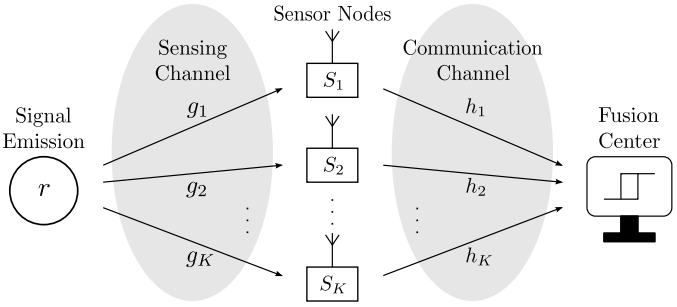

Fig. 1. Abstract representation of the distributed sensor network.

The optimal power allocation for sensor networks, which are used for passive radar applications, has been recently investigated analytically in [1] and subsequently extended in [16] with joint power constraints. This solution includes a total power limitation for the entire sensor network as well as an individual maximum-power limitation for each SN. However, a limitation of the minimum transmission power for each SN is not investigated, such that least reliable SNs remain inactive and cannot participate in the sensing task. To ensure for incessant and reliable radar sensing, especially crucial

The material in this paper was presented in part at the IEEE Wireless Sensor Systems Workshop [1], Baltimore, Maryland, November 2013.

All authors are with the Institute for Theoretical Information Technology, RWTH Aachen University, 52056 Aachen, Germany (e-mail: {alirezaei,taghizadeh,mathar}@ti.rwth-aachen.de).

This article has been accepted for publication in a future issue of this journal, but has not been fully edited. Content may change prior to final publication. Citation information: DOI 10.1109/JSEN.2014.2331271, IEEE Sensors Journal

for signal-tracking and localization, an additional optimization constraint must be included into the power optimization problem for keeping all unreliable SNs in an operating mode with a predefined minimum activity. Moreover, since the main content of [16] targets at finding a theoretical solution to the power allocation problem, it ignores practical limitations and parameter uncertainties, e.g., perfect versus imperfect channel-state knowledge. It is obvious that imperfect parameter knowledge impairs the radar quality. But the specific value of the deterioration depends on the underlying method of power allocation and is sensitive to different system parameters. Thus, the impact of parameter uncertainties is highly important for development and implementation, and must be carefully studied.

In this publication, we consider a sensor network where each SN receives a signal from a jointly observed target source. The particular information about the target signal at each SN is sent to a fusion center, which combines the local observations into a single reliable one. This setup is illustrated in Figure 1 whose technical components will be specified later. In order to avoid functional complexity of SNs and to obtain a simple system model, each SN is assumed to be an amplify-and-forward unit. Both the sensing and the communication channels are subject to additive noise. The fusion center applies a linear fusion rule to combine the distributed local observations. The average deviation between the estimated and the actual signal is utilized as a metric for defining the objective function. Based on this system-setup we solve the power allocation problem analytically. A sum-power constraint and individual minimum and maximum transmission power constraints per SN are considered. The power allocation problem leads to a signomial program, and is analytically solved in closed-form by a Lagrangian setup. This leads to an explicit policy for the optimal power allocation provided that all system parameters are perfectly known. Furthermore, we numerically investigate the behavior of the proposed optimal power allocation when the practical system is subject to parameter inaccuracies and uncertainties. Solving the power allocation problem under the new set of constraints and discussing its sensitivity against parameter imprecision are the main contributions of the present paper.

This paper starts with an overview of the underlying technical system in the next section. Subsequently, the power allocation problem is specified and analytically solved. Finally, the achieved solution is numerically discussed and compared.

Mathematical Notations:

Throughout this paper, we denote the sets of natural, integer, real and complex numbers by $\mathbb{N}$, $\mathbb{Z}$, $\mathbb{R}$ and $\mathbb{C}$, respectively. Note that the set of natural numbers does not include the element zero. Moreover, $\mathbb{R}_+$ denotes the set of non-negative real numbers. Furthermore, we use the subset $\mathbb{F}_N \subseteq \mathbb{N}$, which is defined as $\mathbb{F}_N \coloneqq \{1, \ldots, N\}$ for any given natural number N. We denote the absolute value of a real or complex-valued number z by $|z|$. We also denote the cardinality (number of elements) of a finite set $\mathbb{K}$ by $|\mathbb{K}|$. The expected value of a random variable v is denoted by $\mathcal{E}[v]$. Moreover, the notation

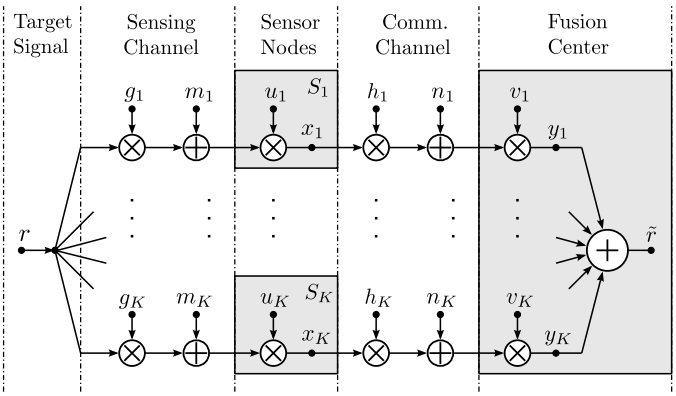

Fig. 2. System model of the distributed sensor network.

$V^\star$ stands for the value of an optimization variable V where the optimum is attained. Finally, vectors and matrices are represented in bold typeface.

II. Overview and Technical System Description

In the following, we shortly describe the underlying system model that is depicted in Figure 2. The continuous-time system is modeled by its discrete-time baseband equivalent, where the sampling rate of the corresponding signals is equal to the target observation rate, for the sake of simplicity. Moreover, we disregard time delays within all transmissions and assume synchronized data communication. A detailed description and specification of the whole system can be found in [16].

At any instance of time, a network of $K \in \mathbb{N}$ independent and spatially distributed sensors receives random observations. If a target signal $r \in \mathbb{C}$ with $R \coloneqq \mathcal{E}[|r|^2]$ and $0 < R < \infty$ is present, then the received power at SN S_k is a part of the emitted power from the target source. Each received signal is weighted by the corresponding channel coefficient $g_k \in \mathbb{C}$ and is disturbed by additive white Gaussian noise (AWGN) $m_k \in \mathbb{C}$ with $M_k \coloneqq \mathcal{E}[|m_k|^2] < \infty$. We assume that the coherence time of all sensing channels is much longer than the whole length of the classification process. Thus, the expected value and the quadratic mean of each coefficient during each observation step can be assumed to be equal to their instantaneous values, i.e., $\mathcal{E}[g_k] = g_k$ and $\mathcal{E}[|g_k|^2] = |g_k|^2$. Furthermore, the channel coefficients as well as the disturbances are assumed to be uncorrelated and jointly independent. The sensing channel is obviously wireless.

All SNs continuously take samples from the disturbed received signal and amplify them by $u_k \in \mathbb{R}_+$ without any additional data processing. Thus, the output signal and the expected value of its instantaneous power are described by

$$x_k \coloneqq (r g_k + m_k) u_k \,, \; k \in \mathbb{F}_K \tag{1}$$

and

$$X_k \coloneqq \mathcal{E}[|x_k|^2] = (R|g_k|^2 + M_k) u_k^2 \,, \; k \in \mathbb{F}_K \,, \tag{2}$$

respectively. The local measurements are then transmitted to a fusion center which is placed in a remote location. The communication to the fusion center is performed by using distinct waveforms for each SN so as to distinguish the

This article has been accepted for publication in a future issue of this journal, but has not been fully edited. Content may change prior to final publication. Citation information: DOI 10.1109/JSEN.2014.2331271, IEEE Sensors Journal

communication of different SNs. Each waveform has to be suitably chosen in order to suppress inter-user (inter-node) interference at the fusion center. Hence, all K received signals at the fusion center are pairwise uncorrelated and are assumed to be conditionally independent. Each received signal at the fusion center is also weighted by the corresponding channel coefficient $h_k \in \mathbb{C}$ and is disturbed by additive white Gaussian noise $n_k \in \mathbb{C}$ with $N_k \coloneqq \mathcal{E}[|n_k|^2] < \infty$, as well. We also assume that the coherence time of all communication channels is much longer than the whole length of the classification process. Thus, the expected value and the quadratic mean of each coefficient during each observation step can be assumed to be equal to their instantaneous values, i.e., $\mathcal{E}[h_k] = h_k$ and $\mathcal{E}[|h_k|^2] = |h_k|^2$. Furthermore, the channel coefficients as well as the disturbances are assumed to be uncorrelated and jointly independent. The data communication between each SN and the fusion center can either be wireless or wired.

The noisy received signals at the fusion center are weighted by $v_k \in \mathbb{C}$ and combined together in order to obtain a single reliable observation $\tilde{r}$ of the actual target signal r. In this way, we obtain

$$y_k \coloneqq \big((r g_k + m_k) u_k h_k + n_k\big) v_k \,, \;\; k \in \mathbb{F}_K \,, \tag{3}$$

and hence,

$$\tilde{r} \coloneqq \sum_{k=1}^{K} y_k = r \sum_{k=1}^{K} g_k u_k h_k v_k + \sum_{k=1}^{K} (m_k u_k h_k + n_k) v_k \,. \tag{4}$$

Note that the fusion center can separate the input streams because the data communication is either wired or performed by distinct waveforms for each SN.

In order to obtain a single reliable observation at the fusion center, the value $\tilde{r}$ should be a good estimate of the present target signal r. Thus, the amplification factors u_k and the weights v_k should be chosen such as to minimize the average absolute deviation between $\tilde{r}$ and the true target signal r. The corresponding optimization program is elaborated in the next section.

A. Some remarks on the system model

Accurate information about all channel coefficients g_k and h_k is needed to determine the optimum power allocation. In many cases it is hard to properly estimate all parameters. Nevertheless, all conclusions from the present investigations may be taken as a bound on what can be achieved by a passive radar system. Moreover, the sensitivity analysis in Section IV shows which deviations are to be expected if parameters are misestimated.

Since the coherence time of communication and sensing channels is assumed to be much longer than the duration of the classification process, the proposed power allocation method is applicable only for scenarios with slow fading channels.

Note that only the linear fusion rule together with the proposed objective function enable optimizing the power allocation in closed-form. The optimum power allocation for other policies is in general hard to determine.

In order to distinguish different modes of operation for each SN, we say that a SN is *inactive* or *idle* if the allocated power is zero. We say a SN is *active* if the allocated power is positive. If a SN is allocated with the minimum output power limitation, i.e., $X_k = P_{\text{min}}$, we say the SN operates with *minimum awareness*. Finally, we say a SN is *saturated* if its allocated power is equal to the maximum output power limitation, i.e., $X_k = P_{\text{max}}$.

An overview of all notations that we will use hereinafter and are needed for the description of each observation process is depicted in Table I.

III. Power Optimization

In this section, we first introduce the power optimization problem and subsequently develop its analytical solution. To solve the optimization problem we apply the general method of Lagrangian multipliers with equality constraints as well as Karush-Kuhn-Tucker (KKT) conditions, see [17, p. 323–335] and [18, p. 243–244].

A. The optimization problem

As mentioned in the last section, the value $\tilde{r}$ should be a good estimate for the present target signal r. In particular, we aim at finding estimators $\tilde{r}$ of minimum mean squared error in the class of unbiased estimators for each r.

The estimate $\tilde{r}$ is unbiased simultaneously for each r if $\mathcal{E}[\tilde{r} - r] = 0$, i.e., from equation (4) we obtain the identity

$$\sum_{k=1}^{K} g_k u_k h_k v_k = 1 \,. \tag{5}$$

This identity is our first constraint in what follows. Note that the mean of the second sum in (4) vanishes since the noise is zero-mean. Furthermore, we do not consider the impact of both random variables g_k and h_k as well as their estimates in our calculations because the coherence time of both channels is assumed to be much longer than the target observation time. Note that equation (5) is complex-valued and may be separated as

$$\sum_{k=1}^{K} u_k |v_k g_k h_k| \cos(\vartheta_k + \phi_k) = 1 \tag{6}$$

and

$$\sum_{k=1}^{K} u_k |v_k g_k h_k| \sin(\vartheta_k + \phi_k) = 0 \,, \tag{7}$$

where ϑ_k and ϕ_k are phases of v_k and $g_k h_k$, respectively.

The average power consumption of each node is approximately equal to its average output power X_k, if the input signal is negligible in comparison to the output signal and if the nodes have smart power components with low-power dissipation loss. We assume that equality between X_k and the average power consumption of each node is ensured. In the present work, we assume that the average output power-range of each SN is limited by $P_{\text{min}} \in \mathbb{R}_+$ and $P_{\text{max}} \in \mathbb{R}_+$ with $0 \leq P_{\text{min}} < P_{\text{max}}$. Furthermore, the average power consumption of all SNs together is assumed to be limited by the sum-power constraint P_{tot} with $K P_{\text{min}} \leq P_{\text{tot}} \leq K P_{\text{max}}$. Hence, the

This article has been accepted for publication in a future issue of this journal, but has not been fully edited. Content may change prior to final publication. Citation information: DOI 10.1109/JSEN.2014.2331271, IEEE Sensors Journal

constraints

$$P_{\text{min}} \leq X_k \leq P_{\text{max}} \quad \Leftrightarrow \; P_{\text{min}} \leq (R|g_k|^2 + M_k)u_k^2 \leq P_{\text{max}}\,, \; k \in \mathbb{F}_K \tag{8}$$

and

$$\sum_{k=1}^{K} X_k \leq P_{\text{tot}} \;\Leftrightarrow\; \sum_{k=1}^{K}(R|g_k|^2 + M_k)u_k^2 \leq P_{\text{tot}} \tag{9}$$

arise consequently. Note that $P_{\text{min}} > 0$ is essential for a gapless radar coverage to enable localization and tracking while the sum-power constraint P_{tot} is a reasonable approach to compare energy-efficient radar systems.

The objective is to minimize the mean squared error $\mathcal{E}[|\tilde{r} - r|^2]$. By using equation (4) and the identity (5) we may write the objective function as

$$V \coloneqq \mathcal{E}\left[|\tilde{r} - r|^2\right] = \sum_{k=1}^{K}\big(M_k u_k^2 |h_k|^2 + N_k\big)|v_k|^2\,. \tag{10}$$

Note that (10) is only valid if m_k and n_k are white and jointly independent.

In summary, the optimization problem is to minimize the mean squared error in (10) with respect to u_k and v_k, subject to constraints (6), (7), (8) and (9). Note that the optimization problem is a *signomial program*, which is a generalization of *geometric programming*, and is thus non-convex in general, see [19].

B. Optimum power allocation

In order to solve the optimization problem, we use the method of Lagrangian multipliers and obtain the corresponding constrained Lagrange function (relaxation with respect to the range of u_k and $|v_k|$) as

$$\begin{aligned} &L(u_k, |v_k|, \vartheta_k; \eta_1, \eta_2, \mu_k, \lambda_k, \tau; \rho_k, \varrho_k, \xi) \\ &\quad\coloneqq \sum_{k=1}^{K}\big(M_k u_k^2 |h_k|^2 + N_k\big)|v_k|^2 \\ &\quad\quad + \left(1 - \sum_{k=1}^{K} u_k |v_k g_k h_k| \cos(\vartheta_k + \phi_k)\right)\eta_1 \\ &\quad\quad - \sum_{k=1}^{K} u_k |v_k g_k h_k| \sin(\vartheta_k + \phi_k)\eta_2 \\ &\quad\quad + \sum_{k=1}^{K}\big(-P_{\text{min}} - \rho_k + (R|g_k|^2 + M_k)u_k^2\big)\mu_k \\ &\quad\quad + \sum_{k=1}^{K}\big(P_{\text{max}} - \varrho_k - (R|g_k|^2 + M_k)u_k^2\big)\lambda_k \\ &\quad\quad + \left(P_{\text{tot}} - \xi - \sum_{k=1}^{K}(R|g_k|^2 + M_k)u_k^2\right)\tau\,, \end{aligned} \tag{11}$$

where η_1, η_2, μ_k, λ_k and τ are Lagrange multipliers while ρ_k, ϱ_k and ξ are slack variables.

Equation (7) is only then satisfied, if all phases $\vartheta_k + \phi_k$ are equal to $q_k\pi$, $q_k \in \mathbb{Z}$, for all $k \in \mathbb{F}_K$. If there were a better solution for $\vartheta_k + \phi_k$, then the first partial derivatives of L with respect to ϑ_k would vanish for that solution, due to the continuity of trigonometric functions. But the first derivatives would lead to equations $\eta_1 \sin(\vartheta_k + \phi_k) = \eta_2 \cos(\vartheta_k + \phi_k)$ which cannot simultaneously satisfy both equations (6) and (7) for all η_1 and η_2. Thus, $q_k\pi$ is the unique solution. Hence, we may consequently write a modified Lagrange function as

$$\begin{aligned} &\tilde{L}(u_k, |v_k|, q_k; \eta_1, \mu_k, \lambda_k, \tau; \rho_k, \varrho_k, \xi) \\ &\quad\coloneqq \sum_{k=1}^{K}\big(M_k u_k^2 |h_k|^2 + N_k\big)|v_k|^2 \\ &\quad\quad + \left(1 - \sum_{k=1}^{K} u_k |v_k g_k h_k| \cos(q_k\pi)\right)\eta_1 \\ &\quad\quad + \sum_{k=1}^{K}\big(-P_{\text{min}} - \rho_k + (R|g_k|^2 + M_k)u_k^2\big)\mu_k \\ &\quad\quad + \sum_{k=1}^{K}\big(P_{\text{max}} - \varrho_k - (R|g_k|^2 + M_k)u_k^2\big)\lambda_k \\ &\quad\quad + \left(P_{\text{tot}} - \xi - \sum_{k=1}^{K}(R|g_k|^2 + M_k)u_k^2\right)\tau\,. \end{aligned} \tag{12}$$

At any stationary point of $\tilde{L}$, all first partial derivatives with respect to each $|v_k|$ and η_1 must vanish, if they exist. This leads to

$$\begin{aligned} \frac{\partial \tilde{L}}{\partial |v_l|} &= 2\big(M_l u_l^2 |h_l|^2 + N_l\big)|v_l| \\ &\quad - \eta_1 u_l |g_l h_l| \cos(q_l\pi) = 0\,, \; l \in \mathbb{F}_K\,, \end{aligned} \tag{13}$$

and

$$\frac{\partial \tilde{L}}{\partial \eta_1} = 1 - \sum_{k=1}^{K} u_k |v_k g_k h_k| \cos(q_k\pi) = 0\,. \tag{14}$$

By multiplying (13) with $|v_l|$, summing up the outcome over all l, and using the identities (6) and (10), we obtain

$$\eta_1 = 2V \tag{15}$$

which is a positive real number due to definition of V. Because of the last relationship and according to (13), the value of $\cos(q_k\pi)$ must be a positive number and hence each q_k must be an even integer number. Thus, we can choose $q_k^\star = 0$ for all $k \in \mathbb{F}_K$ without loss of generality and conclude

$$\vartheta_k^\star = -\phi_k\,, \; k \in \mathbb{F}_K\,. \tag{16}$$

This solution gives the identity $\cos(q_k^\star\pi) = 1$ which can be incorporated into (13) and (14).

From (13), we deduce the equation

$$|v_l| = \frac{\eta_1}{2}\frac{u_l |g_l h_l|}{M_l u_l^2 |h_l|^2 + N_l}\,. \tag{17}$$

Incorporating (17) into (14) yields the relationship

$$\frac{\eta_1}{2} = \left(\sum_{k=1}^{K}\frac{u_k^2 |g_k h_k|^2}{M_k u_k^2 |h_k|^2 + N_k}\right)^{-1}. \tag{18}$$

In turn, we replace $\frac{\eta_1}{2}$ in (17) with (18) and obtain

$$|v_l| = \frac{u_l |g_l h_l|}{M_l u_l^2 |h_l|^2 + N_l}\left(\sum_{k=1}^{K}\frac{u_k^2 |g_k h_k|^2}{M_k u_k^2 |h_k|^2 + N_k}\right)^{-1}. \tag{19}$$

This article has been accepted for publication in a future issue of this journal, but has not been fully edited. Content may change prior to final publication. Citation information: DOI 10.1109/JSEN.2014.2331271, IEEE Sensors Journal

TABLE I
NOTATION OF SYMBOLS THAT ARE NEEDED FOR THE DESCRIPTION OF EACH OBSERVATION PROCESS.

Notation	Description
K	number of all nodes;
$\mathbb{F}_K$	the index-set of K nodes;
$\mathbb{K}_{\text{max}}$	the index-set of all saturated nodes;
$\mathbb{K}_{\text{min}}$	the index-set of all nodes with minimum awareness;
$\mathbb{K}_{\text{lin}}$	the index-set of all nodes within the output power range;
r, R	target signal and its quadratic absolute mean;
$\tilde{r}$	the estimate of r;
g_k, h_k	complex-valued channel coefficients;
m_k, n_k	complex-valued zero-mean AWGN;
M_k, N_k	variances of m_k and n_k;
u_k, v_k	non-negative amplifications and complex-valued weights;
ϑ_k	phase of v_k;
ϕ_k	phase of $g_k h_k$;
y_k	input signals of the combiner;
X_k	output power of k^{th} SN;
P_{min}	minimum output power of each SN;
P_{max}	maximum output power of each SN;
P_{tot}	sum-power constraint.

Note that for each feasible u_k, $k \in \mathbb{F}_K$, equation (19) describes a feasible value for each $|v_k|$. Since for each $u_k > 0$ the relation $|v_k| > 0$ consequently follows, the feasible optimal values of each $|v_k| > 0$ are not on the boundary $|v_k| = 0$. Thus, finding optimal values for each u_k, $k \in \mathbb{F}_K$, leads to optimum values for each $|v_k|$, $k \in \mathbb{F}_K$, due to the convexity of (11) with respect to each $|v_k|$. Hence, finding a unique global optimum for u_k, $k \in \mathbb{F}_K$, yields the sufficient condition for the globally optimal solution of the minimization problem (11).

By considering (15) and (18), we deduce the identity

$$V = \frac{\eta_1}{2} = \left(\sum_{k=1}^{K} \frac{u_k^2 |g_k h_k|^2}{M_k u_k^2 |h_k|^2 + N_k} \right)^{-1}, \tag{20}$$

where the objective and η_1 consequently are described in terms of u_k. For the sake of simplicity and in order to compare the results later on, we define two new quantities as

$$\alpha_k \coloneqq \sqrt{\frac{|g_k|^2}{M_k}} \;\Rightarrow\; \alpha_k \in \mathbb{R}_+ , \tag{21}$$

and

$$\beta_k \coloneqq \sqrt{\frac{N_k (R|g_k|^2 + M_k)}{M_k |h_k|^2}} \;\Rightarrow\; \beta_k \in \mathbb{R}_+ . \tag{22}$$

By using the new quantities as well as (2), the equation (20) is equivalent to

$$V = \frac{\eta_1}{2} = \left(\sum_{k=1}^{K} \frac{\alpha_k^2 X_k}{X_k + \beta_k^2} \right)^{-1} . \tag{23}$$

Since the minimization of the objective V in (23) is equivalent to the minimization of $\tilde{V} \coloneqq -V^{-1}$, we only consider the objective $\tilde{V}$ in the following. Initially, we highlight three important properties of $\tilde{V}$. First, the new objective function is strictly decreasing with respect to each X_k, $k \in \mathbb{F}_K$, which can easily be seen from the representation

$$\tilde{V} = -\sum_{k=1}^{K} \frac{\alpha_k^2}{1 + \beta_k^2 / X_k} . \tag{24}$$

Second, the objective function is twice differentiable with respect to each X_k, $k \in \mathbb{F}_K$, because its first and second derivatives exist. Third, the objective function is a jointly convex function with respect to $(X_k)_{k \in \mathbb{F}_K}$ which can be shown by calculating the corresponding Hessian $\mathbf{H} \coloneqq (\frac{\partial^2 \tilde{V}}{\partial X_k \partial X_l})_{k,l \in \mathbb{F}_K}$. The Hessian is positive-definite because of

$$\mathbf{z}' \mathbf{H} \mathbf{z} = \sum_{k=1}^{K} \frac{2 \alpha_k^2 \beta_k^2 z_k^2}{(X_k + \beta_k^2)^3} > 0 , \quad \forall\ \mathbf{z} \coloneqq (z_1, z_2, \ldots, z_K)' \in \mathbb{R}^K \setminus \{\mathbf{0}\} . \tag{25}$$

By considering (2), we obtain that the remaining sum-power constraint in (12) is linear and thus also jointly convex with respect to $(X_k)_{k \in \mathbb{F}_K}$. Hence, we are able to define a modified convex minimization problem by the unconstrained Lagrangian

$$\begin{aligned} \hat{L}(X_k;\, \mu_k, \lambda_k, \tau) \coloneqq & -\sum_{k=1}^{K} \frac{\alpha_k^2 X_k}{X_k + \beta_k^2} + \sum_{k=1}^{K} (P_{\text{min}} - X_k) \mu_k \\ & + \sum_{k=1}^{K} (-P_{\text{max}} + X_k) \lambda_k + \left(-P_{\text{tot}} + \sum_{k=1}^{K} X_k \right) \tau , \end{aligned} \tag{26}$$

where again μ_k, λ_k and τ are Lagrange multipliers. Note that the Lagrange multiplier η_1 is positive because of (15), and the equality $\sin(\vartheta_k^\star + \phi_k) = 0$ holds due to (16). Hence, both constraints (6) and (7) are discarded in (26). Furthermore, the sum-power constraint can be considered as an equality constraint instead of an inequality constraint due to monotonicity of the objective, see also complementary slackness theorem [18].

In order to solve the new convex optimization problem in (26), we apply the KKT-conditions which are sufficient for optimality in convex problems. These conditions are as follows for any optimal point $(X_k^\star, \mu_k^\star, \lambda_k^\star, \tau^\star)$:

$$\begin{aligned} X_l^\star &\geq P_{\text{min}} , && l \in \mathbb{F}_K , && \text{(27a)} \\ X_l^\star &\leq P_{\text{max}} , && l \in \mathbb{F}_K , && \text{(27b)} \\ \mu_l^\star &\geq 0 , && l \in \mathbb{F}_K , && \text{(27c)} \\ \lambda_l^\star &\geq 0 , && l \in \mathbb{F}_K , && \text{(27d)} \\ (P_{\text{min}} - X_l^\star) \mu_l^\star &= 0 , && l \in \mathbb{F}_K , && \text{(27e)} \\ (P_{\text{max}} - X_l^\star) \lambda_l^\star &= 0 , && l \in \mathbb{F}_K , && \text{(27f)} \\ \sum_{k=1}^{K} X_k^\star &= P_{\text{tot}} , && && \text{(27g)} \end{aligned}$$

and

$$\frac{\partial \hat{L}}{\partial X_l} = -\frac{\alpha_l^2 \beta_l^2}{(X_l^\star + \beta_l^2)^2} - \mu_l^\star + \lambda_l^\star + \tau^\star = 0, \quad l \in \mathbb{F}_K . \tag{27h}$$

If $X_l^\star = P_{\text{min}}$ for some $l \in \mathbb{F}_K$, then from (27c), (27f) and (27h) the inequality $\frac{1}{\sqrt{\tau^\star}} \leq \frac{P_{\text{min}} + \beta_l^2}{\alpha_l \beta_l}$ follows. If $X_l^\star = P_{\text{max}}$ for some $l \in \mathbb{F}_K$, then from (27d), (27e) and (27h) the inequality $\frac{1}{\sqrt{\tau^\star}} \geq \frac{P_{\text{max}} + \beta_l^2}{\alpha_l \beta_l}$ follows. If $P_{\text{min}} < X_l^\star < P_{\text{max}}$, then from (27e), (27f) and (27h) both the equality $X_l^\star = \alpha_l \beta_l \big(\frac{1}{\sqrt{\tau^\star}} - \frac{\beta_l}{\alpha_l} \big)$ and the double

This article has been accepted for publication in a future issue of this journal, but has not been fully edited. Content may change prior to final publication. Citation information: DOI 10.1109/JSEN.2014.2331271, IEEE Sensors Journal

inequality $P_{\min} < \frac{\alpha_l \beta_l}{\sqrt{\tau^\star}} - \beta_l^2 < P_{\max}$ follow. In summary, we may write

$$X_k^\star = \max\Big\{P_{\min}, \min\Big\{P_{\max}, \alpha_k\beta_k\Big(\chi^\star - \frac{\beta_k}{\alpha_k}\Big)\Big\}\Big\},\ k \in \mathbb{F}_K, \tag{28}$$

where χ is a replacement for $\frac{1}{\sqrt{\tau}}$ and is called *water-level*. In order to calculate the transmission power of each SN from (28) we first have to determine the water-level. Unfortunately, the water-level can only be determined if the operation mode of each SN is somehow known. Therefore, we have to separate all SNs into three groups. The first group contains all SNs, which are saturated, and is denoted by the subset $\mathbb{K}_{\max}$. The second group contains all SNs, which operate within their output power-range, and is denoted by the subset $\mathbb{K}_{\text{lin}}$. The third group contains all other SNs, which operate with minimum awareness, and is denoted by $\mathbb{K}_{\min}$. Note that all subsets are pairwise disjoint and their union is the subset of all SNs, i.e.,

$$\mathbb{K}_{\max} \coloneqq \{k \in \mathbb{F}_K \mid X_k^\star = P_{\max}\}, \tag{29a}$$
$$\mathbb{K}_{\min} \coloneqq \{k \in \mathbb{F}_K \mid X_k^\star = P_{\min}\} \tag{29b}$$

and

$$\begin{aligned}\mathbb{K}_{\text{lin}} &\coloneqq \{k \in \mathbb{F}_K \mid P_{\min} < X_k^\star < P_{\max}\} \\ &= \mathbb{F}_K \setminus (\mathbb{K}_{\max} \cup \mathbb{K}_{\min})\,.\end{aligned} \tag{29c}$$

Furthermore, because of the above discussion, the subsets in (29) are equivalent to

$$\mathbb{K}_{\max} = \Big\{k \in \mathbb{F}_K \mid \tfrac{P_{\min}+\beta_k^2}{\alpha_k\beta_k} \geq \chi^\star\Big\}, \tag{30a}$$
$$\mathbb{K}_{\min} = \Big\{k \in \mathbb{F}_K \mid \tfrac{P_{\max}+\beta_k^2}{\alpha_k\beta_k} \leq \chi^\star\Big\} \tag{30b}$$

and

$$\mathbb{K}_{\text{lin}} = \Big\{k \in \mathbb{F}_K \mid \tfrac{P_{\min}+\beta_k^2}{\alpha_k\beta_k} < \chi^\star < \tfrac{P_{\max}+\beta_k^2}{\alpha_k\beta_k}\Big\} \tag{30c}$$

which simultaneously provide necessary and sufficient conditions to select the specific subset for each SN. If the membership of each SN is specified by one of the above subsets, the water-level follows by (28) from (27g) as

$$\begin{aligned}\chi^\star &= \frac{P_{\text{tot}} - \sum\limits_{k\in\mathbb{K}_{\max}} P_{\max} - \sum\limits_{k\in\mathbb{K}_{\min}} P_{\min} + \sum\limits_{k\in\mathbb{K}_{\text{lin}}} \beta_k^2}{\sum\limits_{k\in\mathbb{K}_{\text{lin}}} \alpha_k\beta_k} \\ &= \frac{P_{\text{tot}} - |\mathbb{K}_{\max}|P_{\max} - |\mathbb{K}_{\min}|P_{\min} + \sum\limits_{k\in\mathbb{K}_{\text{lin}}} \beta_k^2}{\sum\limits_{k\in\mathbb{K}_{\text{lin}}} \alpha_k\beta_k} \\ &= \frac{P'_{\text{tot}} - |\mathbb{K}_{\max}|P'_{\max} + \sum\limits_{k\in\mathbb{K}_{\text{lin}}} (\beta_k^2 + P_{\min})}{\sum\limits_{k\in\mathbb{K}_{\text{lin}}} \alpha_k\beta_k}\end{aligned} \tag{31}$$

with $P'_{\text{tot}} \coloneqq P_{\text{tot}} - KP_{\min}$ and $P'_{\max} \coloneqq P_{\max} - P_{\min}$. In the following, we want to present the efficient Algorithm 1 which optimally separates all SNs into the correct subsets $\mathbb{K}_{\max}$, $\mathbb{K}_{\min}$ and $\mathbb{K}_{\text{lin}}$. Note that the proposed algorithm can be implemented more efficiently, but for sake of comprehensibility, we have chosen the given representation. Since Algorithm 1 is an adapted version of an algorithm proposed and proved in [16], we refer the reader to the paper [16] for a detailed proof.

Algorithm 1 Separation of sensor nodes

$\mathbb{K}_{\max} \leftarrow \emptyset$
$P_{\text{remain}} \leftarrow P'_{\text{tot}}$
repeat
  $\mathbb{K}_{\text{lin}} \leftarrow \mathbb{F}_K \setminus \mathbb{K}_{\max}$
  repeat
    $\chi \leftarrow \frac{P_{\text{remain}} + \sum_{k\in\mathbb{K}_{\text{lin}}} (\beta_k^2 + P_{\min})}{\sum_{k\in\mathbb{K}_{\text{lin}}} \alpha_k\beta_k}$ ▷ see (31)
    $X_k \leftarrow \alpha_k\beta_k\big(\chi - \frac{\beta_k}{\alpha_k}\big),\ k \in \mathbb{K}_{\text{lin}}$ ▷ see (28)
    $\mathbb{K}_- \leftarrow \{k \in \mathbb{K}_{\text{lin}} \mid X_k \leq P_{\min}\}$ ▷ see (29b)
    $\mathbb{K}_{\text{lin}} \leftarrow \mathbb{K}_{\text{lin}} \setminus \mathbb{K}_-$
  until $\mathbb{K}_- = \emptyset$ **or** $\mathbb{K}_{\text{lin}} = \emptyset$
  $\mathbb{K}_+ \leftarrow \{k \in \mathbb{K}_{\text{lin}} \mid X_k \geq P_{\max}\}$ ▷ see (29a)
  $\mathbb{K}_{\max} \leftarrow \mathbb{K}_{\max} \cup \mathbb{K}_+$
  $P_{\text{remain}} \leftarrow P_{\text{remain}} - |\mathbb{K}_+|P'_{\max}$
until $\mathbb{K}_+ = \emptyset$ **or** $\mathbb{K}_{\max} = \mathbb{F}_K$
$\mathbb{K}_{\text{lin}} \leftarrow \mathbb{K}_{\text{lin}} \setminus \mathbb{K}_+$
$\mathbb{K}_{\min} \leftarrow \mathbb{F}_K \setminus (\mathbb{K}_{\max} \cup \mathbb{K}_{\text{lin}})$
return $(\mathbb{K}_{\max}, \mathbb{K}_{\text{lin}}, \mathbb{K}_{\min})$

First, the results from (31) and (28) are applied in the inner loop to achieve an optimal solution neglecting the output power-range constraint $P_{\max}$. In the first repetition, this is performed on all SNs and in each further repetition on all SNs included in the subset $\mathbb{K}_{\text{lin}}$. At the end of the inner loop, the subset $\mathbb{K}_+$ contains all SNs which operate at their output power-range limitation $P_{\max}$. They are added to the subset of all saturated SNs $\mathbb{K}_{\max}$. At last, the power used by those SNs is subtracted from the available sum-power which gives the remaining sum-power P_{remain}. With these updated settings, the procedure is repeated until the subset $\mathbb{K}_+$ of saturated SNs is empty. Note that both $\mathbb{K}_{\min}$ and $\mathbb{K}_{\max}$ might be empty. It can be shown that the water-level, and thereby, the power for each non-saturated SN is increasing in each repetition of the outer loop. Thus, it is possible that SNs with minimum awareness may loose their current operating mode, and hence, all non-saturated SNs are potential candidates to achieve a better operating mode. In contrast, the water-level is decreasing in each repetition of the inner loop. Thus, neglecting the output power-range constraint $P_{\max}$ in the inner loop is meaningful and obvious. Finally, we obtain the (optimal) subsets of SNs to continue solving the optimization problem in (26).

After determination of $\mathbb{K}_{\max}$, $\mathbb{K}_{\min}$ and $\mathbb{K}_{\text{lin}}$, we use (31) to calculate $\chi^\star$, and in turn, by inserting $\chi^\star$ into (28) we obtain $X_k^\star$. Subsequently from (2), (19) and (23), we infer

$$u_k^\star = \sqrt{\frac{P_{\max}}{R|g_k|^2 + M_k}}\,,\ k \in \mathbb{K}_{\max}\,, \tag{32}$$

$$u_k^\star = \sqrt{\frac{P_{\min}}{R|g_k|^2 + M_k}}\,,\ k \in \mathbb{K}_{\min}\,, \tag{33}$$

This article has been accepted for publication in a future issue of this journal, but has not been fully edited. Content may change prior to final publication. Citation information: DOI 10.1109/JSEN.2014.2331271, IEEE Sensors Journal

$$u_k^\star = \sqrt{\frac{1}{M_k|h_k|^2}\left(\chi^\star\sqrt{\frac{|g_k h_k|^2 N_k}{R|g_k|^2+M_k}}-N_k\right)},\ k\in\mathbb{K}_{\text{lin}}\,, \tag{34}$$

$$V^\star = \left(\sum_{k\in\mathbb{K}_{\max}}\frac{\alpha_k^2 P_{\max}}{P_{\max}+\beta_k^2}+\sum_{k\in\mathbb{K}_{\min}}\frac{\alpha_k^2 P_{\min}}{P_{\min}+\beta_k^2}+\sum_{k\in\mathbb{K}_{\text{lin}}}\alpha_k^2\left(1-\frac{\beta_k}{\chi^\star\alpha_k}\right)\right)^{-1} \tag{35}$$

and

$$|v_k^\star| = \frac{V^\star u_k^\star |g_k h_k|}{M_k(u_k^\star)^2|h_k|^2+N_k}\,,\ k\in\mathbb{F}_K\,. \tag{36}$$

The equations (16), (28) and (32)–(36) together with (31) and Algorithm 1 describe the optimal solution of the power allocation problem and hence are the main contribution of the present subsection.

C. Discussion of the solution

By using the results from Subsection III-B, all K SNs are active if $P_{\min}>0$ is pre-defined. In contrast, if $P_{\min}=0$ is the requested case, then only $|\mathbb{K}_{\max}|+|\mathbb{K}_{\text{lin}}|$ SNs are active and participate in the data fusion. In general, all SNs, which are members of $\mathbb{K}_{\max}$, are more reliable than those which are members of $\mathbb{K}_{\text{lin}}$. In turn, SNs, which are members of $\mathbb{K}_{\text{lin}}$, are more reliable than those which are members of $\mathbb{K}_{\min}$. The reliability of each SN is determined by the corresponding ratio $\frac{\beta_k}{\alpha_k}$ that can be interpreted as *interference-power*, see equation (28). The SN with the smallest interference-power is the most reliable one while the SN with the greatest interference-power is the least reliable one among all SNs. This means that for the identification of the most reliable SNs in a certain network, that can be modeled as depicted in Figure 2, only the ratios $\frac{\beta_k}{\alpha_k}$ are important. Hence, sorting all SNs by their interference-power yields an easy selection method of most reliable SNs for practical applications. In summary we can conclude that SNs with smaller interference-power are allocated with more available sum-power than those with greater interference-power.

By using the amplification factors from (32)–(34) and the weights from (16) and (36), the single observation $\tilde{r}$ is an estimator of minimum mean squared error in the class of unbiased estimators for the target signal r. Hence, we obtain the estimate

$$\tilde{r} = r+\sum_{k=1}^{K}(m_k u_k^\star h_k+n_k)v_k^\star \tag{37}$$

from (4). The above equation shows that $\tilde{r}$ is equal to r with some additional noise. Hence, $\tilde{r}-r$ is a zero-mean Gaussian random variable with an absolute variance of $V^\star$, see (35). Note that $\tilde{r}$ is an unbiased estimator for r due to constraint (5). By similar methods we can also minimize the mean squared error without restricting ourself to unbiased estimators. Obviously, the optimal value of V will then be smaller than that in (35).

Note that the obtained results are quite similar but not identical to the well-known *water-filling* solution, see [20]. The distinction arises from our definition of the water-level χ which differs from the general description.

TABLE II
DEFAULT VALUES OF ALL PARAMETERS USED FOR EACH REFERENCE CURVE.

Parameter	Default value
K	20
R	1
σ_g^2	2
σ_h^2	2
$\sigma_{\Delta g}^2$	0
$\sigma_{\Delta h}^2$	0
M_0	2
N_0	2
$P_{\min}$	0.1
$P_{\max}$	2
P_{tot}	10

IV. SENSITIVITY ANALYSIS

In this section, we first simulatively investigate the behavior of the optimal value in (35), with respect to $|g_k|^2$, $|h_k|^2$, M_k and N_k. For the sake of simplicity, we use $\sigma_g^2 \coloneqq \mathcal{E}[|g_k|^2]$, $\sigma_h^2 \coloneqq \mathcal{E}[|h_k|^2]$, $M_0 \coloneqq \mathcal{E}[|m_k|^2]$ and $N_0 \coloneqq \mathcal{E}[|n_k|^2]$ hereinafter. Subsequently, we analyze the sensitivity of a sensor network, which is indeed designed by the optimal strategy of power allocation from Subsection III-B, but with an imperfect knowledge about the channel-state. In particular, we investigate different independent cases, where in turn the estimates $\hat{g}_k \coloneqq g_k+\Delta g_k$ and $\hat{h}_k \coloneqq h_k+\Delta h_k$ are used instead of g_k and h_k itself, respectively, in order to re-design the power allocation of the same sensor network. Afterwards, we compare the optimal value in (35) of the sensor network with optimal known parameters to the conditional mean square error (MSE)

$$\hat{V} \coloneqq \mathcal{E}\left[|\tilde{r}-r|^2 \mid \Delta g_k, \Delta h_k\right] \tag{38}$$

of the re-designed sensor network with imperfect information. In general, the estimate $\tilde{r}$ in (38) is biased compared to the case with perfect information, i.e., $\mathcal{E}[\tilde{r}-r]\neq 0$. In addition, the selection of most reliable SNs is no longer ensured. Hence, the value in (38) is mostly greater than that of (35), see also the definition (10). Furthermore, due to inaccurate knowledge of sensing channels, the given power constraints may be violated in the erroneous design. All these effects are equivalently relevant for a discussion and comparison. Since an analytical comparison seems to be out of reach, we set out to use numerical methods to obtain the sensitivity analysis and visualize corresponding simulation results.

In order to fairly compare all results, we simulate a *reference* curve for each figure. All reference curves are based on parameters under consideration with default values given in Table II. Unless otherwise stated, we usually create a new curve only by changing the value of a single parameter. The specific new value of that parameter is noted in the legend of the corresponding figure. All random processes g_k, h_k, Δg_k, Δh_k, m_k, n_k and r are randomly generated with zero mean Gaussian distributions for each simulation step. All other parameters are kept constant. The number of iterations per simulation point is always 100000.

This article has been accepted for publication in a future issue of this journal, but has not been fully edited. Content may change prior to final publication. Citation information: DOI 10.1109/JSEN.2014.2331271, IEEE Sensors Journal

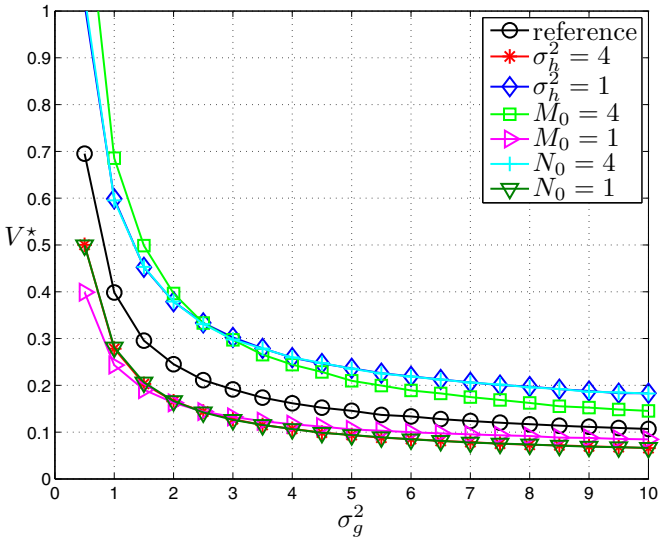

Fig. 3. Behavior of $V^\star$ with respect to the variance σ_g^2 of sensing channels. All curves show a decreasing property in σ_g^2. The reference curve has the default parameters $\sigma_h^2 = 2$, $M_0 = 2$ and $N_0 = 2$.

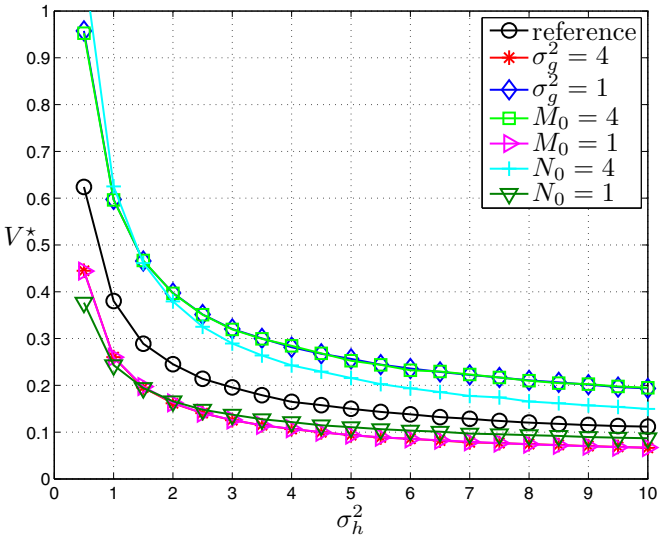

Fig. 4. Behavior of $V^\star$ with respect to the variance σ_h^2 of communication channels. All curves show a decreasing property in σ_h^2. The reference curve has the default parameters $\sigma_g^2 = 2$, $M_0 = 2$ and $N_0 = 2$.

A. Behavior of $V^\star$

In Figure 3, the decreasing property of $V^\star$ with respect to the variance σ_g^2 of all sensing channels is shown. The reason behind the decreasing property is that the whole network observes the target signal more reliable for higher variances of sensing channels. Furthermore, it can be seen that increasing N_0 has an equivalent effect on the objective as decreasing σ_h^2 and vice versa. It is also interesting to note that the objective shows highest sensitivity to the variation of M_0 when the sensing channel is rather weak (small σ_g^2). The observed sensitivity is reduced for higher variances of sensing channels. Furthermore, the objective attains a more or less constant value for very high variances of the sensing channel. The reason is that the resulted objective is dominated by the quality of the communication channel when the sensing channel gets stronger.

Figure 4 illustrates that $V^\star$ is also decreasing with respect to the variance σ_h^2 of all communication channels. Since the diversity of the communication channel is high for a high value of σ_h^2, the data communication to the fusion center is consequently better which results in a lower $V^\star$. Analogously, increasing M_0 is equivalent to decreasing σ_g^2 and vice versa. Similar to the discussion of the sensing channel, the resulted objective becomes rather constant for a high quality of communication channels, since the sensitivity of the objective is already dominated by the quality of sensing channels and a further improvement of the communication quality is rather unimportant. This also results in a higher sensitivity of $V^\star$ with respect to the sensing quality based on σ_g^2 and M_0 for the region of high σ_h^2.

In Figure 5 it is shown that in contrast to the curves in Figure 3 and Figure 4, the property of $V^\star$ is increasing with respect to the noise power M_0 and all curves behave almost linear. The deviation of all curves is greater for large values of M_0 than for small values. Furthermore, the value of M_0 has more impact on the deviation of $V^\star$ caused by σ_g^2 than by other parameters, as mentioned before. As already described for Figure 3 and Figure 4, increasing N_0 is equivalent to decreasing σ_h^2 and vice versa.

From Figure 6 we observe that $V^\star$ is also increasing with respect to the noise power N_0. In general, all curves show a similar behavior compared to those curves in Figure 5.

B. Sensitivity of $\hat{V}$

A sensitivity analysis of $\hat{V}$ is very important in order to justify assumptions concerning the channel-state knowledge. In Figure 7, we consider the case where the error variance $\sigma_{\Delta g}^2 := \mathcal{E}[|\Delta g_k|^2]$ of estimated sensing channels is greater than

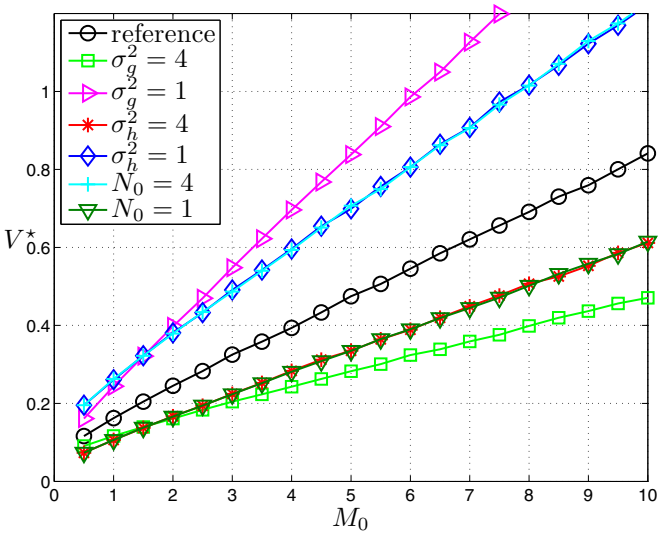

Fig. 5. Behavior of $V^\star$ with respect to the variance M_0 of noise signals. All curves show an increasing property in M_0. The reference curve has the default parameters $\sigma_g^2 = 2$, $\sigma_h^2 = 2$ and $N_0 = 2$.

This article has been accepted for publication in a future issue of this journal, but has not been fully edited. Content may change prior to final publication. Citation information: DOI 10.1109/JSEN.2014.2331271, IEEE Sensors Journal

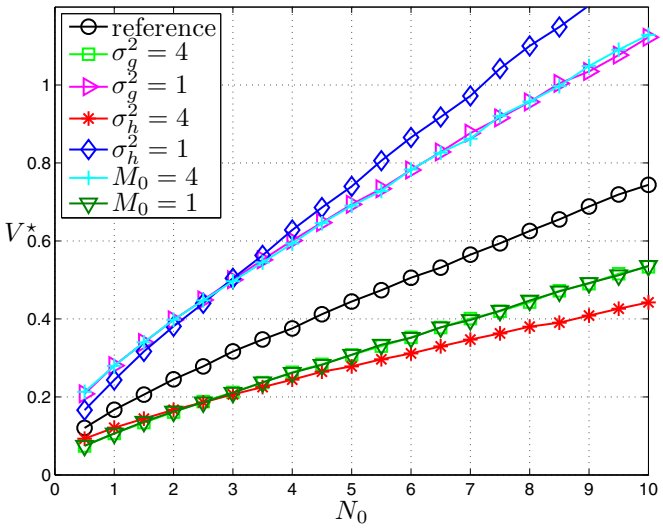

Fig. 6. Behavior of $V^\star$ with respect to the variance N_0 of noise signals. All curves show an increasing property in N_0. The reference curve has the default parameters $\sigma_g^2 = 2$, $\sigma_h^2 = 2$ and $M_0 = 2$.

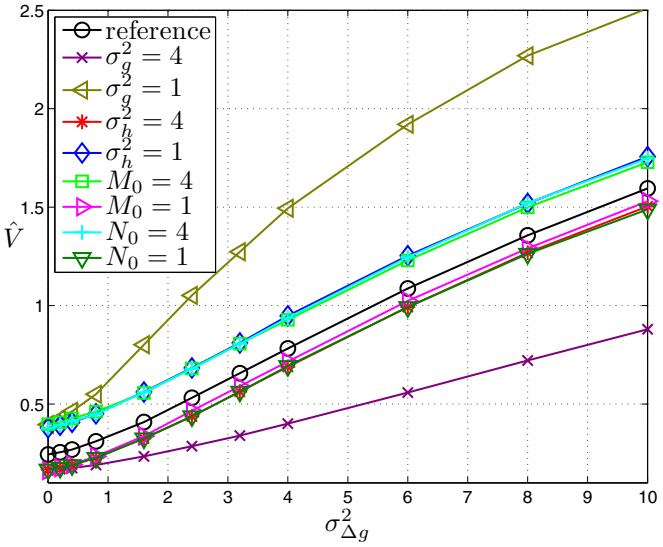

Fig. 7. Behavior of $\hat{V}$ with respect to the variance $\sigma_{\Delta g}^2$ of estimation errors. All curves show an increasing property in $\sigma_{\Delta g}^2$. The reference curve has the default parameters $\sigma_g^2 = 2$, $\sigma_h^2 = 2$, $M_0 = 2$ and $N_0 = 2$.

or equal to zero. In the case where $\sigma_{\Delta g}^2$ is equal to zero, the identity $\hat{V} = V^\star$ holds. Otherwise, $\hat{V}$ is always greater than $V^\star$, i.e., $\hat{V}(\sigma_{\Delta g}^2) \geq \hat{V}(0)$. All curves pass through three different regions whereas only the first and the second region are visible in Figure 7. In the first region, i.e., for low values of $\sigma_{\Delta g}^2$, all curves are slowly increasing. The selection of most reliable SNs is still mostly ensured in the first region while the optimal power allocation is no longer insured. In the second region, i.e., for mid-range values of $\sigma_{\Delta g}^2$, all curves are rapidly increasing since the correct sensor selection gets out of control. In the last region, i.e., for high values of $\sigma_{\Delta g}^2$, all curves are linearly increasing. In this region the optimal sensor selection almost always fails. This means that SNs are randomly selected and the allocated power is also random. The increasing property (not constant) of all curves in the third region is comparable with the increasing property in the first region, because the roles of g_k and Δg_k are exchanged. The system is designed by Δg_k instead of g_k and thus g_k itself acts as an estimation error of Δg_k. In summary, the best operation region of the proposed system is the first region in which $\sigma_{\Delta g}^2 \ll \sigma_g^2$ holds, while a system operation in the third region, for which $\sigma_{\Delta g}^2 \gg \sigma_g^2$ holds, should be avoided. As can also be seen, the deterioration of the performance is not only amplified by high noise powers M_0 and N_0, but also by low channel variances σ_g^2 and σ_h^2. The form of the curves is mainly dominated and prescribed by the channel variance σ_g^2. All curves in the middle of the figure run almost parallel because the variance σ_g^2 of all those curves is the same.

In Figure 8, the other case is depicted in which the estimation of the communication channel is noisy. Analogously, if the variance $\sigma_{\Delta h}^2 := \mathcal{E}[|\Delta h_k|^2]$ of estimation error is equal to zero, the equality $\hat{V} = V^\star$ holds. In general, all curves again show similar behavior compared to those curves from Figure 7. Interestingly, the curves in Figure 7 achieve mostly a better performance than those in Figure 8. This states that the accurate estimation of all communication channels is more crucial for the system performance than the estimation of the sensing channels. The reason behind this fact can be seen from the righthand side of equation (4). An estimation error in each h_k in connection with wrongly optimized u_k and v_k causes additional noises which cannot be caused by an estimation error in each g_k. This asymmetrical property is beneficial, because the estimation of the sensing channels is in practice very difficult while the estimation of the communication channels can be arbitrarily accurate with the aid of pilot sequences for each SN.

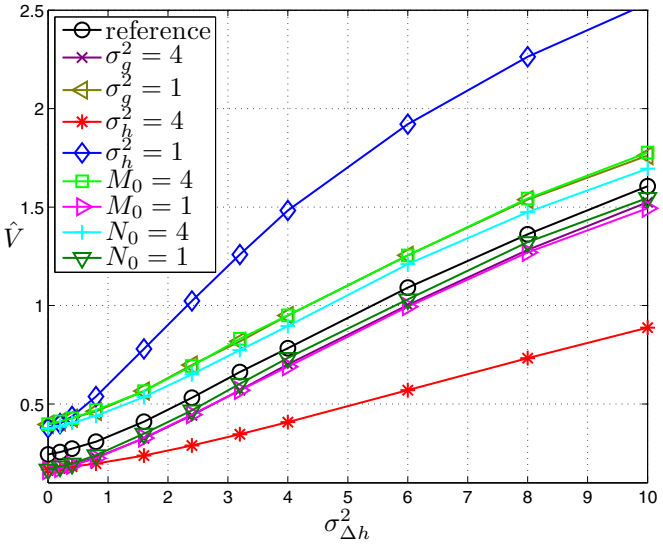

Fig. 8. Behavior of $\hat{V}$ with respect to the variance $\sigma_{\Delta h}^2$ of estimation errors. All curves show an increasing property in $\sigma_{\Delta h}^2$. The reference curve has the default parameters $\sigma_g^2 = 2$, $\sigma_h^2 = 2$, $M_0 = 2$ and $N_0 = 2$.

C. Summary

In case of perfect parameter knowledge, the variation of each parameter shows the behavior of the objective with respect to the parameter under consideration. As it was expected, the objective is decreasing with respect to the variance of each channel coefficient and increasing with respect to the variance of each noise signal. In case of imperfect channel-state information, the mean square error is increasing with respect to the variance of each estimation error. All corresponding results show three functional regions which correspond to the cases '*the selection of more reliable sensor nodes is mostly ensured but the power allocation is suboptimal*', '*a selection of more reliable sensor nodes is no longer guaranteed*' and '*the sensor selection as well as the power allocation are just randomly performed*'. In the first and last region, the curves are slowly increasing while in the second region a drastic increase of the curves is visible. Hence, the first region is the most beneficial region for a non-stop operation of the sensor network. Furthermore, the curves demonstrate that an accurate estimation of communication channels is more important in comparison to the sensing channels. This property is in general very crucial for radar systems, since the sensing channel cannot be accurately estimated.

V. Conclusion

In the present work we have derived an optimal solution to the power allocation problem for distributed passive multiple-radar systems. Three different power constraints have been considered and the corresponding optimal solution in closed-form has been presented. The optimum point is attained when sensor nodes are in one of three possible states, depending on their degree of reliability. An efficient algorithm has been developed to determine the respective optimum states and operating modes of all sensor nodes. Furthermore, we have analyzed the sensitivity of the optimal solution, based on system simulations, by varying the variance of channel coefficients and the noise. Perfect channel-state information is the initial situation, which is compared to inaccurate parameter estimation via the mean squared error. Comprehensive graphical representations support our claim that accurate estimation of communication channels is more important than accurate estimation of sensing channels.

Acknowledgment

This work was inspired by Prof. Dr. sc. techn. H. Meyr. We would like to thank him for his advice and collaboration.

References

[1] G. Alirezaei, R. Mathar, and P. Ghofrani, "Power optimization in sensor networks for passive radar applications," in *The Wireless Sensor Systems Workshop 2013 (WSSW'13) co-located with the IEEE International Conference on Wireless for Space and Extreme Environments (WiSEE'13)*, Baltimore, Maryland, USA, Nov. 2013.

[2] (2010, Dec.) Icecube neutrino observatory. University of Wisconsin-Madison and National Science Foundation. Amundsen-Scott South Pole Station, Antarctica. [Online]. Available: http://icecube.wisc.edu/

[3] (2012, Mar.) The very large array. The National Radio Astronomy Observatory. Socorro County, New Mexico, USA. The National Radio Astronomy Observatory is a facility of the National Science Foundation operated under cooperative agreement by Associated Universities, Inc. [Online]. Available: http://www.vla.nrao.edu/

[4] A. L. Hume and C. J. Baker, "Netted radar sensing," in *Proc. IEEE Int. Radar Conf.*, 2001, pp. 23–26.

[5] I. Immoreev and J. Taylor, "Future of radars," in *Ultra Wideband Systems and Technologies, 2002. Digest of Papers. 2002 IEEE Conference on*, 2002, pp. 197–199.

[6] M. I. Skolnik, *Introduction to Radar Systems*, 3rd ed. New York: McGraw-Hill Higher Education, 2002.

[7] P. K. Varshney, *Distributed Detection and Data Fusion*. New York: Springer, 1997.

[8] F. Meshkati, H. Poor, and S. Schwartz, "Energy-efficient resource allocation in wireless networks," *Signal Processing Magazine, IEEE*, vol. 24, no. 3, pp. 58–68, 2007.

[9] H. Godrich, A. Petropulu, and H. Poor, "Power allocation strategies for target localization in distributed multiple-radar architectures," *Signal Processing, IEEE Transactions on*, vol. 59, no. 7, pp. 3226–3240, 2011.

[10] S. Gezici, Z. Tian, G. B. Giannakis, H. Kobayashi, A. F. Molisch, H. V. Poor, and Z. Sahinoglu, "Localization via ultra-wideband radios: A look at positioning aspects for future sensor networks," *IEEE Signal Process. Mag.*, vol. 22, pp. 70–84, Jul. 2005.

[11] Y. Shen, W. Dai, and M. Win, "Optimal power allocation for active and passive localization," in *Global Communications Conference (GLOBECOM), 2012 IEEE*, 2012, pp. 3713–3718.

[12] A. Høst-Madsen and J. Zhang, "Capacity bounds and power allocation for wireless relay channels," *Information Theory, IEEE Transactions on*, vol. 51, no. 6, pp. 2020–2040, 2005.

[13] M. Emadi, A. Davoodi, and M. Aref, "Analytical power allocation for a full-duplex decode-and-forward relay channel," *Communications, IET*, vol. 7, no. 13, pp. 1338–1347, 2013.

[14] G. Alirezaei and R. Mathar, "Optimum power allocation for sensor networks that perform object classification," in *2013 Australasian Telecommunication Networks and Applications Conference (ATNAC 2013)*, Christchurch, New Zealand, Nov. 2013.

[15] M. Chen, S. Serbetli, and A. Yener, "Distributed power allocation strategies for parallel relay networks," *Wireless Communications, IEEE Transactions on*, vol. 7, no. 2, pp. 552–561, 2008.

[16] G. Alirezaei, M. Reyer, and R. Mathar, "Optimum power allocation in sensor networks for passive radar applications," *Wireless Communications, IEEE Transactions on*, 2014, to be published after June 2014.

[17] D. G. Luenberger and Y. Ye, *Linear and Nonlinear Programming*, 3rd ed. Springer Science+Business Media, 2008.

[18] S. Boyd and L. Vandenberghe, *Convex Optimization*. California: Cambridge University Press, 2004.

[19] M. Chiang, *Geometric Programming for Communication Systems*. Princeton: now Publishers Inc., 2005.

[20] S. Stańczak, M. Wiczanowski, and H. Boche, *Fundamentals of Resource Allocation in Wireless Networks: Theory and Algorithms*, 2nd ed. Berlin: Springer, 2008.